UNIVERSITY OF MINNESOTA

Twin Cities Campus

Saint Anthony Falls Laboratory
Engineering, Environmental, Biological and Geophysical Fluid Dynamics

College of Science and Engineering

Mississippi River at 3rd Avenue S. E.
Minneapolis, MN 55414

Dept. Main Office: 612-624-4363
Fax: 612-624-4398

Project Title: Virtual Wind Simulator with Advanced Control & Aeroelastic Model for Improving the Operation of Wind Farms

Contract Number: RD4-13 **Milestone Number**: 5 **Report Date**: 5/3/2018

Principal Investigator: Fotis Sotiropoulos
(631) 632-8380

Contract Contact: Bridget Foss
(612) 624-5571

Congressional District: (Corporate office) Minnesota 5^{th}

Congressional District: (Project location) Minnesota 5^{th}

MILESTONE REPORT

Executive Summary: The goal for this project is to develop, demonstrate and transfer into practice an industry-leading numerical simulation model for optimization of performance, financial decision making, and operational planning of existing and newly planned wind energy plants. This project will leverage the previously completed Cycle 3 RDF project through which the first version of the Virtual Wind Simulator software (VWiS) was developed and validated. We will extend the capabilities of this first generation modeling tool to include the ability to simulate aeroelastic loading of the blades and incorporate current industry standards and advanced turbine control methods and technologies and we will demonstrate these capabilities via comparisons with data from utility-scale wind turbines and farms. The resulting VWiS+ modeling tool will thus be able to be used in practice to improve wind farm performance and reduce operational costs.

As planned, during this reporting period (monthly) activities have been carried out to address the following objectives:

1. Flow field characterization around the EOLOS wind turbine with existing and improved blade control strategies;

2. Flow field characterization in an Xcel Energy wind farm.

Project funding provided by customers of Xcel Energy through a grant from the Renewable Development Fund.

Technical Progress:

1 Flow field characterization around the EOLOS wind turbine

In the last milestone report, we presented the test plan for validating the load reduction performance of the IPC (individual pitch control) considering different wind conditions. Specifically, the data collected will be categorized based on wind speed, shear and turbulence intensity to fully validate the controller performance under different load cases. Therefore, a met tower wind measurement file will be associated with turbine output data files. The test plan also includes sensor measurements of the blades and tower on the output data list for comprehensive evaluation of the load reduction performance. Three different controllers, i.e., the baseline controller without IPC, the integral controller that targets on only the 1P load on blades and the H-infinity controller that suppresses both the 1P load and 3P loads on the turbine, will be considered.

From 11/02/2017, the data collection in the EOLOS field has been started to evaluate the load reduction performance of the IPC. The SODAR measurements were taken at the EOLOS station in the north of the turbine. Together with the measurements at the meteorological tower, we will be able to measure both incoming wind and turbine wake at the same time for testing the effects of different controllers on turbine wake. On 01/18/2018 the latest version of the firmware was loaded onto the TCU and tested in collective pitch mode for stability. This latest build of firmware introduces a fix to resolve spikes that were observed in blade root moment calculations in the previous build. The SODAR measurements at the EOLOS field station established a baseline for incoming wind and turbine wake when the turbine operates with its standard pitch control algorithm. The collected data from the wind turbine controller are employed to validate that all calculations necessary for the IPC are correct and that the algorithm is robust enough to handle short communication losses and occasional bad data from the strain sensors in the wind turbine blades. Once all the control algorithms have been vetted and all foreseeable scenarios have been tested in simulation, testing of the algorithm on the turbine will commence.

Analysis of the data collected in the EOLOS field will be reported in the next milestone report.

2 SODAR measurement in the Pleasant Valley wind farm

The data collection in the Pleasant Valley wind farm was conducted from March 17, 2017 to October 26, 2017. SODAR (SOnic Detection And Ranging) was employed for measuring the wind speed and wind direction at six different locations in the wind farm. The wind data were measured at $z = 3, 30, 35, 40, 45,\ 50, 55, 60, 65, 70,\ 75, 80, 85, 90, 95, 100, 105,\ 110, 115, 120, 125, 130, 135,$ $140, 145, 150, 155, 160, 165,\ 170, 175, 180, 185, 190, 195, 200$ m above the ground for every minute. The six locations are close to T18, T30, T33, T75, T78 and T96 turbines. The measurements at T18 location were contaminated because of the influence from the surrounding turbines, which will not be analyzed in this report. The measurements at $z = 3$ m are not of interest in this study and will not be analyzed. Table 2.1 shows the measurement period for each location. As seen, the measurement was taken for about a month at each location. The objective of this work is to characterize the wind

Table 2.1: Dates for measurement in the Pleasant Valley wind farm, MN, USA conducted in 2017.

Location	T30	T33	T75	T78	T96
Dates	05/03–06/05	06/07–07/10	07/12–08/14	08/06–09/18	09/19–10/26

in this wind farm especially the turbine wakes and provide dataset for validating computational models.

2.1 Results

We analyze the measured wind data in this section. Figure 2.1 shows the probability density function (PDF) of the wind direction at different vertical positions at the five different locations. As seen the wind directions are almost the same at the $z = 45$, 95 and 145 m locations. At T30 location, the wind mainly blows from 30^o and 120^o wind directions. At T33 location, the wind mainly blows from 345^o and 240^o wind directions. At T75 location, the wind mainly blows from 195^o and 30^o wind directions. At T78 location, the wind mainly blows from 180^o and 315^o wind directions. At T96 location, the wind mainly blows from 165^o and 315^o wind directions.

Figure 2.2 shows the PDF of wind speed from all directions at different vertical positions at the five different measurement locations. The bars are the measured data. The red lines are the Weibull distributions with the coefficients best-fitted from the measured data. The Weibull distribution of wind speed V is expressed as

$$p(V)dV = \frac{k}{c}\left(\frac{V}{c}\right)^{k-1} \exp\left[-\left(\frac{V}{c}\right)^{k}\right] dV \tag{2.1}$$

where c is the scale factor (m/s) and k the shape factor (dimensionless). From figure 2.2, it is seen that the PDFs of wind speed are well represented by the Weibull distribution for all the measurement locations, which corresponds to different day/month during the year and different surrounding turbine layouts. Different values of scale factor c and shape factor k are observed for different measurement locations. At the same location, the shape factor is similar for wind speed distribution at $z = 45, 95$ and 135 m vertical locations. The scale factor is observed to increase with z from $z = 45$ to 135 above the ground.

The vertical variations of the scale factor c and the shape factor k of the best-fitted Weibull distributions for wind speed from all directions are shown in figure 2.3. Different values of c and k are observed for the measurements at five different locations, which were taken during different day/month in the year. However, it is observed that the vertical variations of c and k are similar for different locations. The vertical profiles of c follow a logarithmic relationship with z. The shape factor k gradually increases from $z = 30$ m to about $z = 60$ m and decreases for further vertical positions except for the measurement near T96, which does not show the increase in the near ground

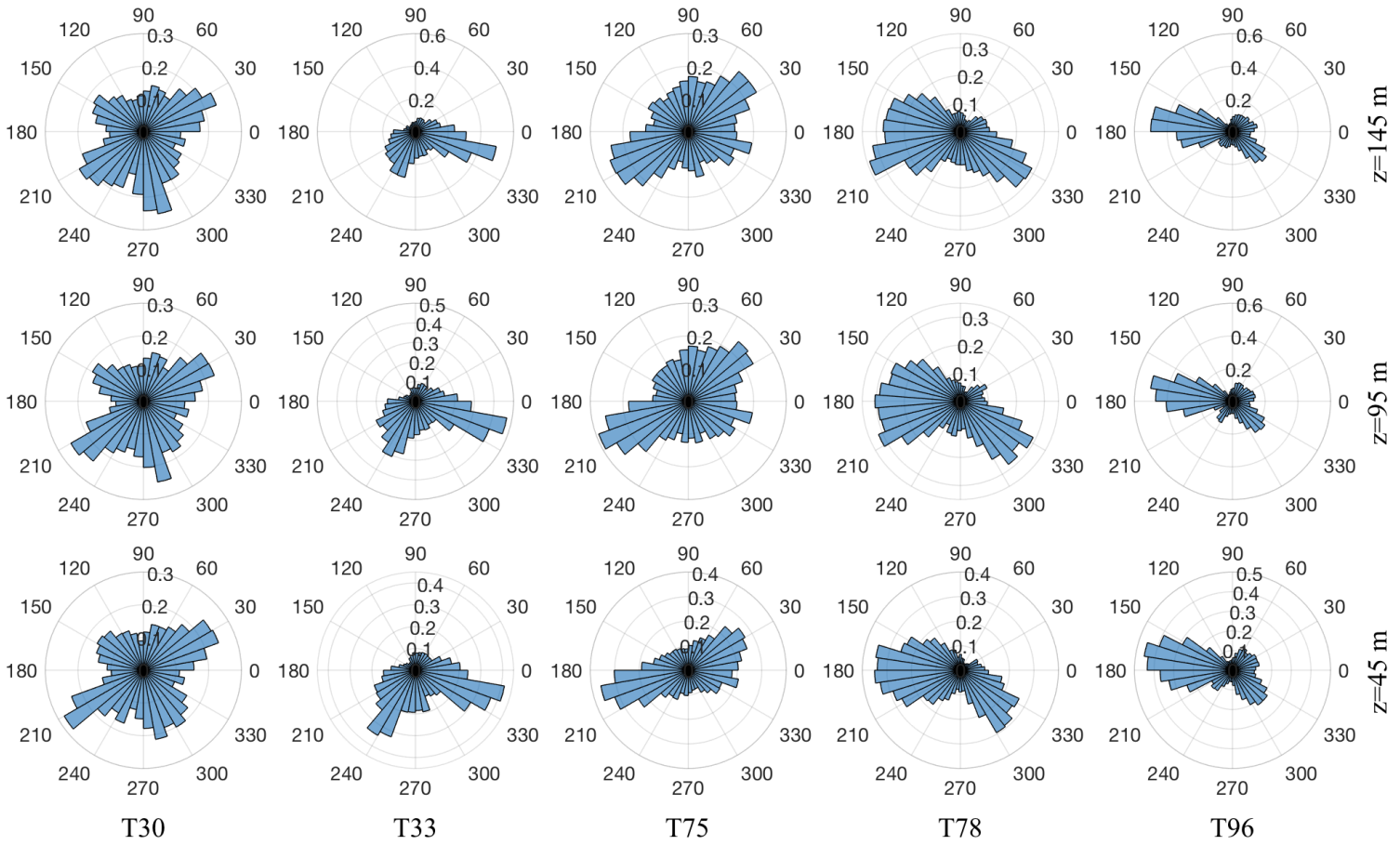

Figure 2.1: PDF of wind direction at $z = 45$ m, $z = 95$ m and $z = 145$ m above the ground for different measurement locations. The figure shows the angle in degrees. It is noticed that the PDF is calculated based on radians instead of degrees.

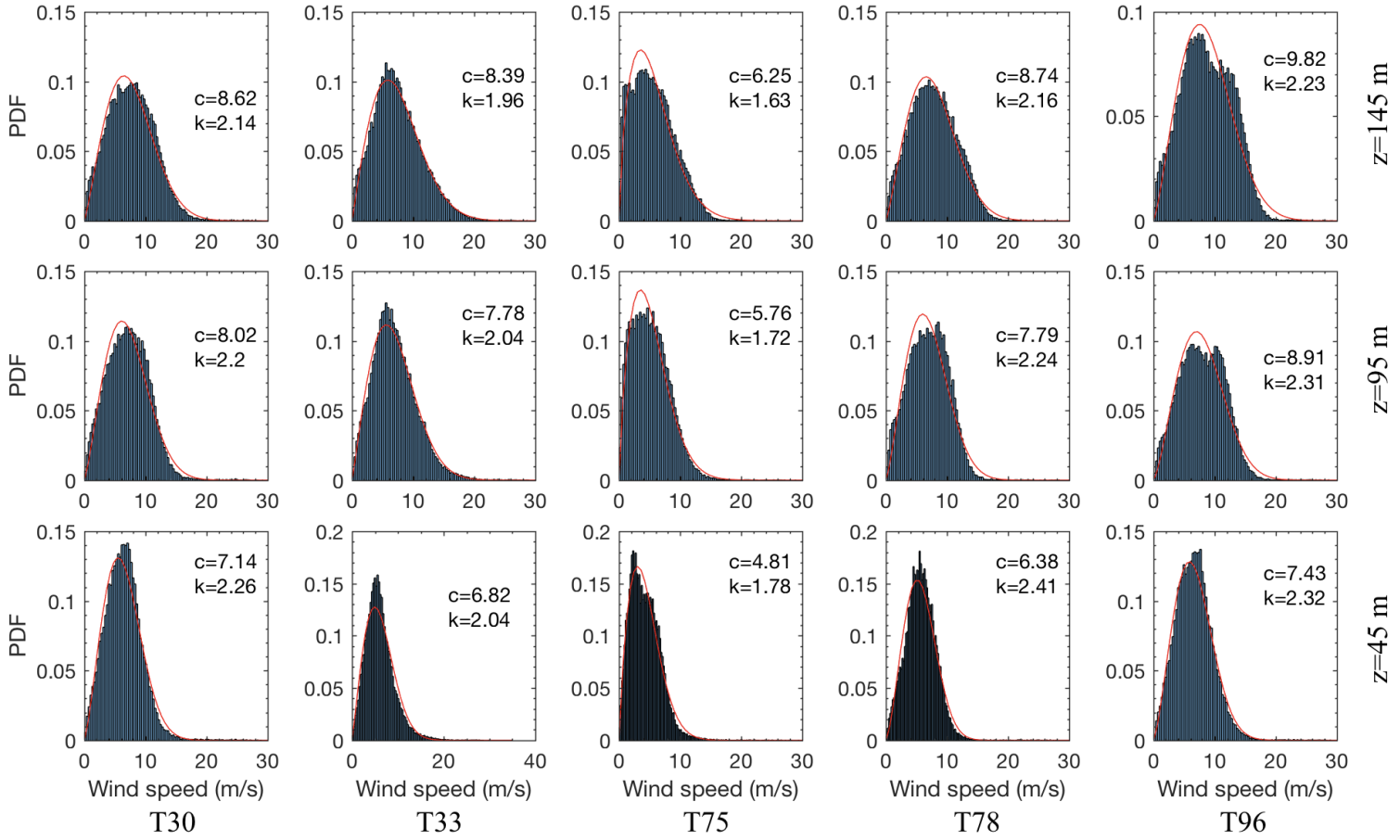

Figure 2.2: PDF of wind speed from all directions at $z = 45$ m, $z = 95$ m and $z = 145$ m above the ground for different measurement locations. The red solid lines are the best-fitted Weibull distributions.

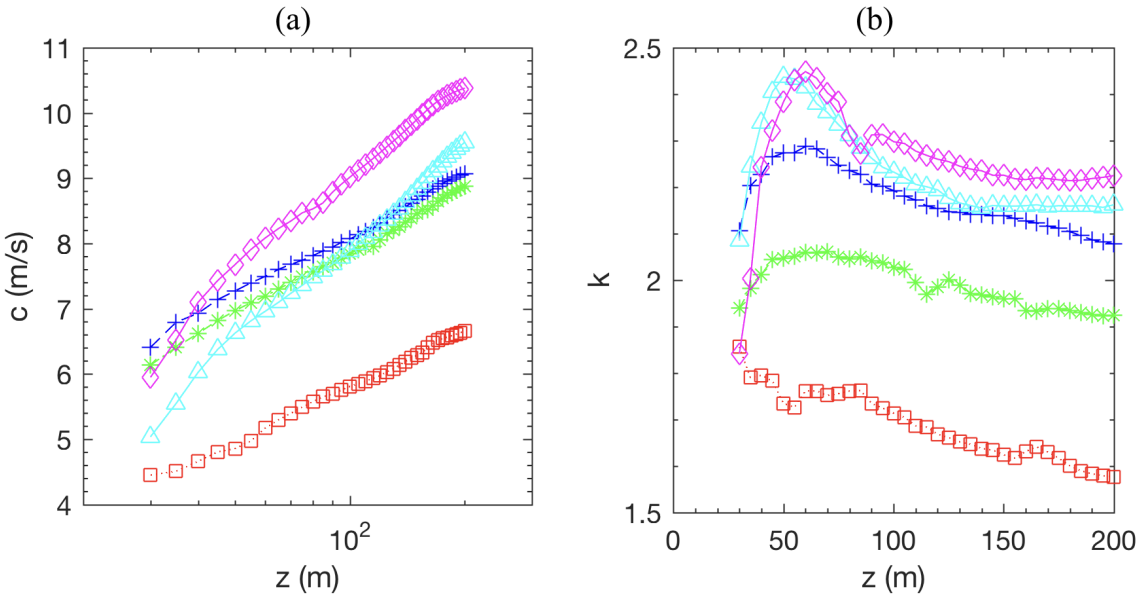

Figure 2.3: Vertical variations of scale factor c and shape factor k of the Weibull distributions best-fitted using the measurement data for different measurement locations. Blue-dashed line with crosses: T30; Green dash-dot line with asterisks: T33; Red dotted line with squares: T75; Cyan solid line with triangles: T78; Magenta solid line with diamonds: T96.

region.

To further analyze the wind characteristics in the Pleasant Valley wind farm, the wind data are divided into 16 parts based on 8 different wind directions, i.e., 0^o, 45^o, 90^o, 135^o, 180^o, 225^o, 270^o and 315^o and day/night. Figures 2.4 and 2.5 show the time-averaged wind speed and scale factor c and shape factor k for the measurements near T30 turbine location, respectively. Different vertical variations of the wind speed are observed for the data measured during day and night at the same location because of different thermal stratifications. Wake profiles are observed when wind blows from the south (180^o). Because of the different profiles of mean wind speed, different values of shape factor c are observed for day and night measurements. It is noticed that the vertical variation of the shape factor is similar to the time-averaged wind speed in the sense that the c in the wake region is lower that that out of the wake. The overall trend in the vertical direction still follows very well the logarithmic relationship for other wind directions without turbine wakes. The values of the shape factor k are significantly different for different wind directions. The shapes of the k profiles are also different from the one shown in figure 2.3 which considers all wind directions.

The vertical profiles of the time-averaged wind speed and Weibull parameters (c and k) for the measurements at other locations are shown in figures. 2.6, 2.8, 2.10 and 2.12 and figures. 2.7, 2.9, 2.11 and 2.13, respectively. Similar trend as that for the measurements near T30 turbine is observed.

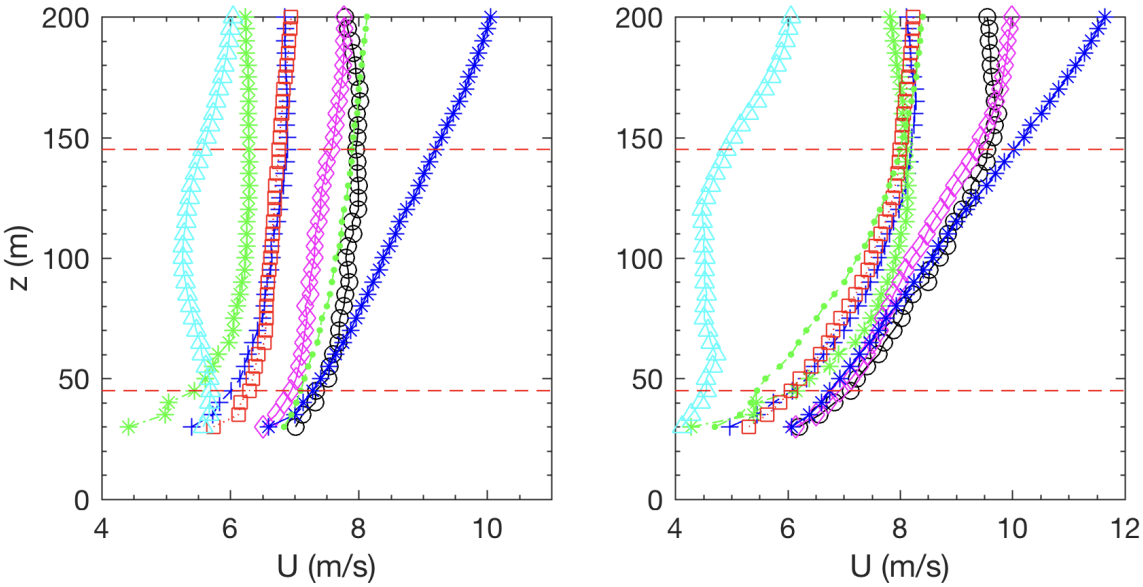

Figure 2.4: Vertical profiles for time-averaged wind speed for different wind directions for wind data measured near the T30 turbine location. Black solid line with circles: 0^o; Blue-dashed line with crosses: 45^o; Green dash-dot line with asterisks: 90^o; Red dotted line with squares: 135^o; Cyan solid line with triangles: 180^o; Magenta solid line with diamonds: 225^o; Blue solid line with asterisks: 270^o; Green dashed line with points: 315^o. Left figures: day measurement; Right figures: night measurement.

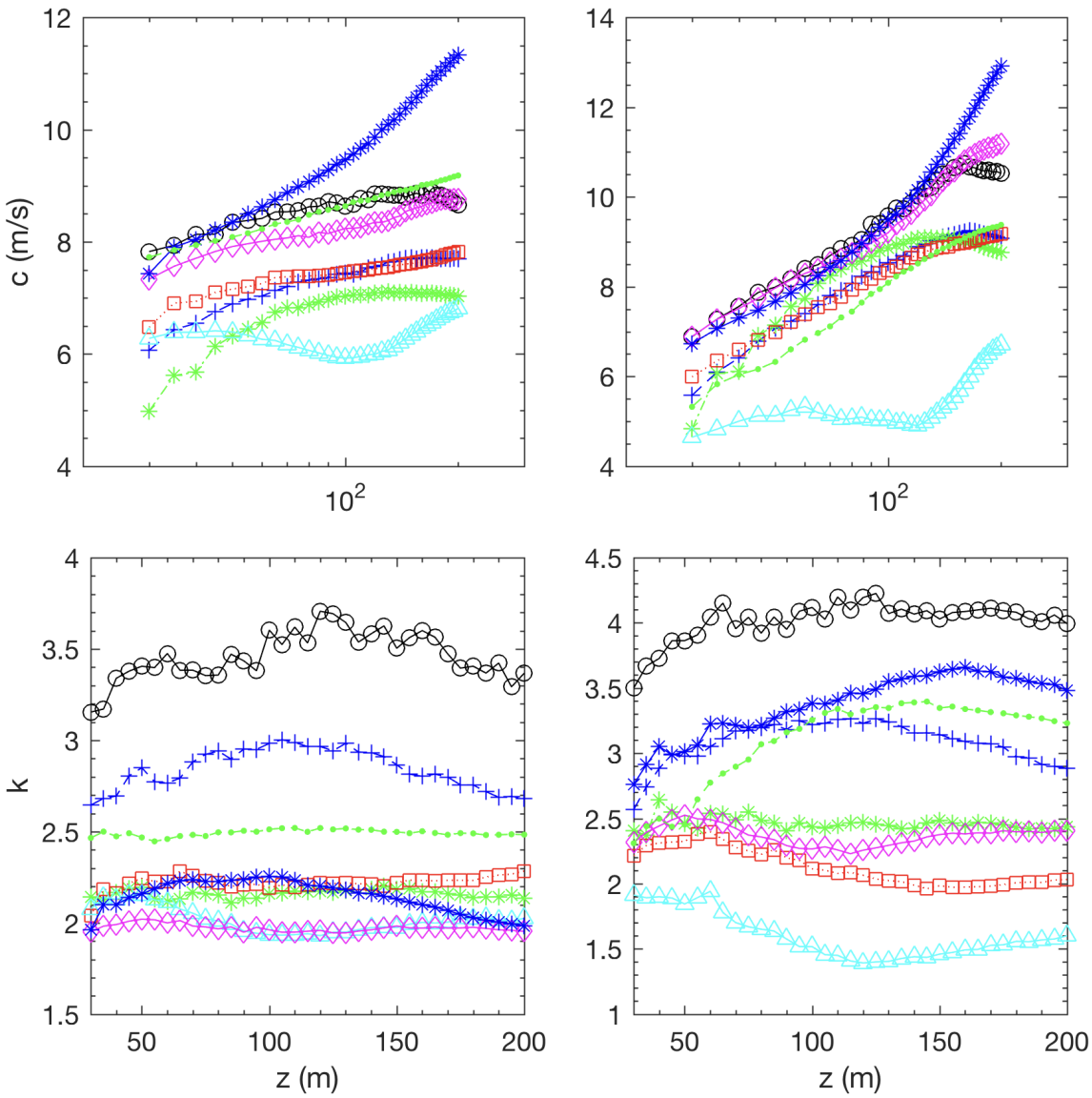

Figure 2.5: Vertical variations of scale factor c and shape factor k of the Weibull distributions best-fitted using the measurement data near T30 turbine for different wind directions. Black solid line with circles: 0^o; Blue-dashed line with crosses: 45^o; Green dash-dot line with asterisks: 90^o; Red dotted line with squares: 135^o; Cyan solid line with triangles: 180^o; Magenta solid line with diamonds: 225^o; Blue solid line with asterisks: 270^o; Green dashed line with points: 315^o. Left figures: day measurement; Right figures: night measurement.

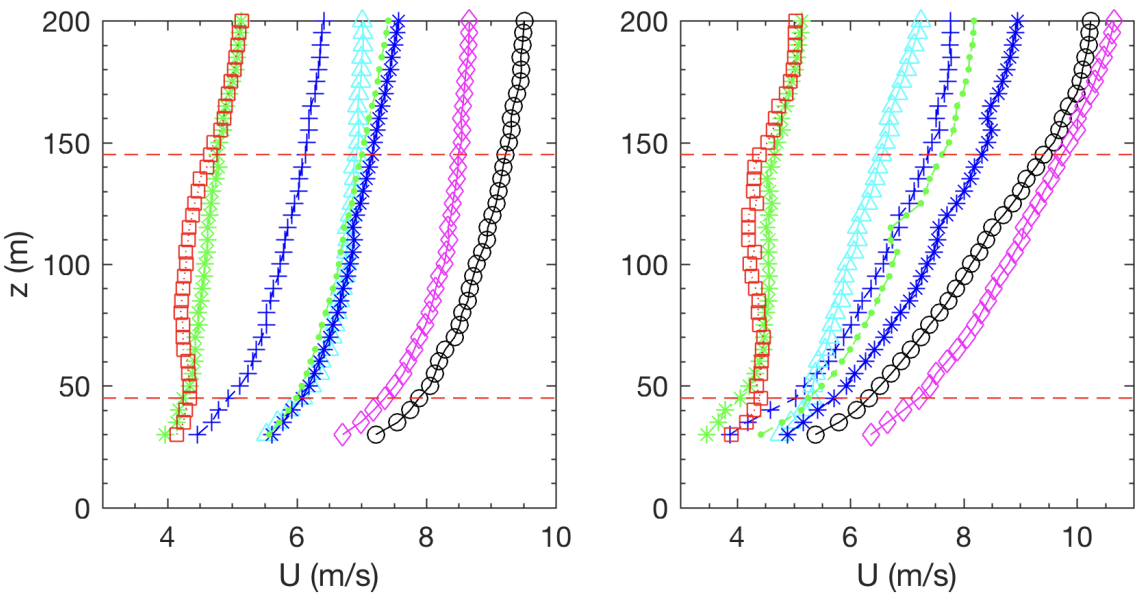

Figure 2.6: Vertical profiles for time-averaged wind speed for different wind directions for wind data measured near the T33 turbine location. Black solid line with circles: 0^o; Blue-dashed line with crosses: 45^o; Green dash-dot line with asterisks: 90^o; Red dotted line with squares: 135^o; Cyan solid line with triangles: 180^o; Magenta solid line with diamonds: 225^o; Blue solid line with asterisks: 270^o; Green dashed line with points: 315^o. Left figures: day measurement; Right figures: night measurement.

We will not further describe them.

In order to investigate how the values of c and k depend on the wind speed, we average the c and k in the vertical location and plot the averaged $< c >$ and $< k >$ as a function of averaged $< U >$ in figure 2.14. It is seen that the $< c >$ linearly increases as a function of $< U >$ with the its values slightly higher than $< U >$ for all the wind directions and measurement locations. The shape factor $< k >$ also increases as a function of $< U >$. However the data are more scattered. The red points show the measurements with turbine wakes. It is seen that the averaged c for measurements with wakes lies on the same line as the other cases. For the shape factors of measurements with wakes, it is seen that the corresponding k values are lower than those without wakes and are nearly the same for all the wake measurements with only one exception.

2.2 Summary of progress 2

In this section, we reported the wind characteristics in the Pleasant Valley wind farm by analyzing the measured SODAR data. We plotted the probability density function distributions of the wind direction and wind speed. We analyzed the wind speed for different wind directions. Wake profiles

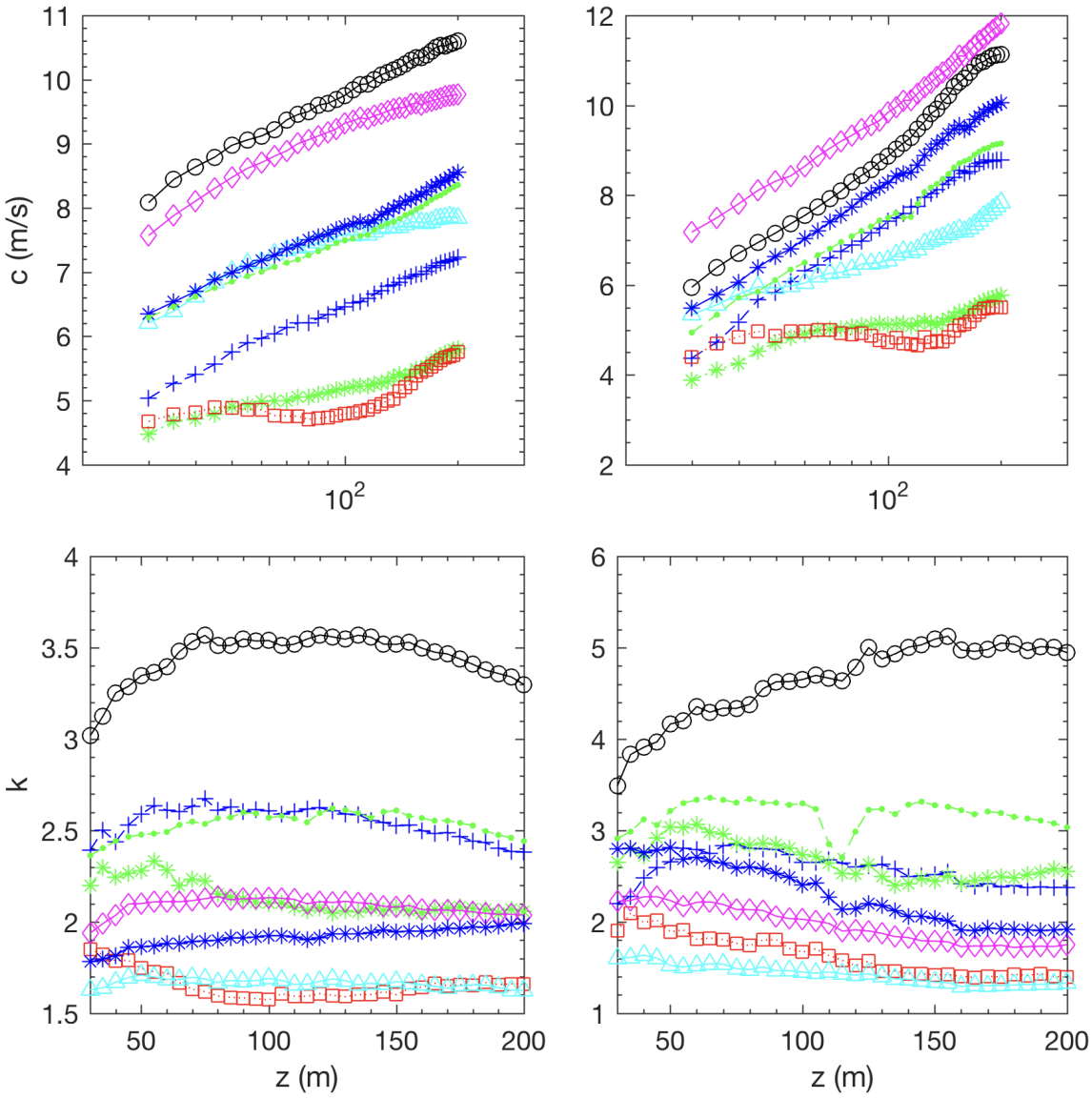

Figure 2.7: Vertical variations of scale factor c and shape factor k of the Weibull distributions best-fitted using the measurement data near T33 turbine for different wind directions. Black solid line with circles: 0^o; Blue-dashed line with crosses: 45^o; Green dash-dot line with asterisks: 90^o; Red dotted line with squares: 135^o; Cyan solid line with triangles: 180^o; Magenta solid line with diamonds: 225^o; Blue solid line with asterisks: 270^o; Green dashed line with points: 315^o. Left figures: day measurement; Right figures: night measurement.

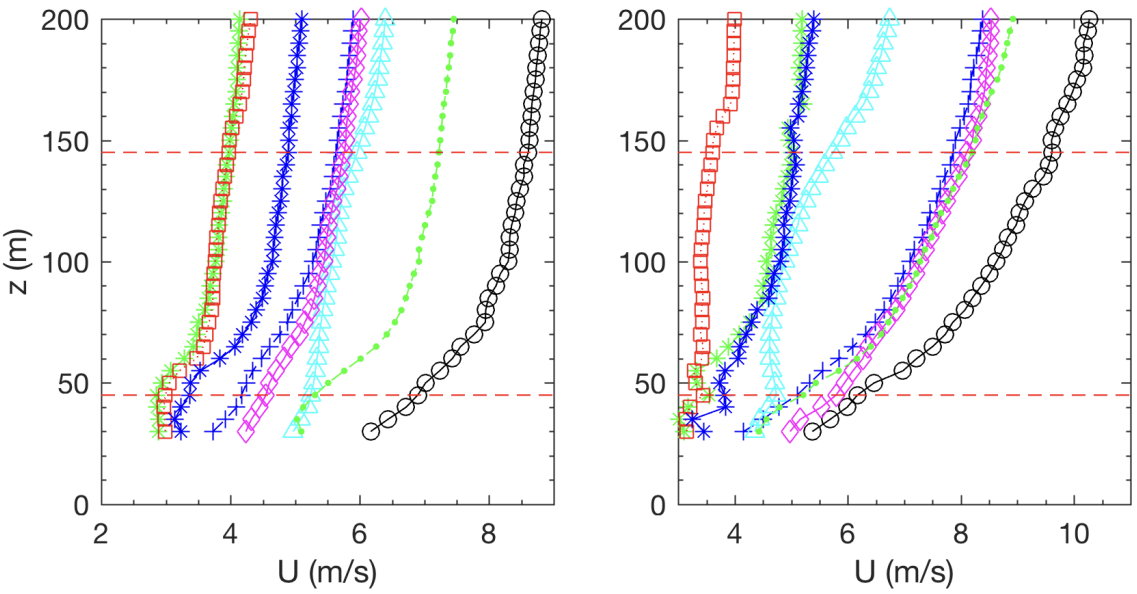

Figure 2.8: Vertical profiles for time-averaged wind speed for different wind directions for wind data measured near the T75 turbine location. Black solid line with circles: 0^o; Blue-dashed line with crosses: 45^o; Green dash-dot line with asterisks: 90^o; Red dotted line with squares: 135^o; Cyan solid line with triangles: 180^o; Magenta solid line with diamonds: 225^o; Blue solid line with asterisks: 270^o; Green dashed line with points: 315^o. Left figures: day measurement; Right figures: night measurement.

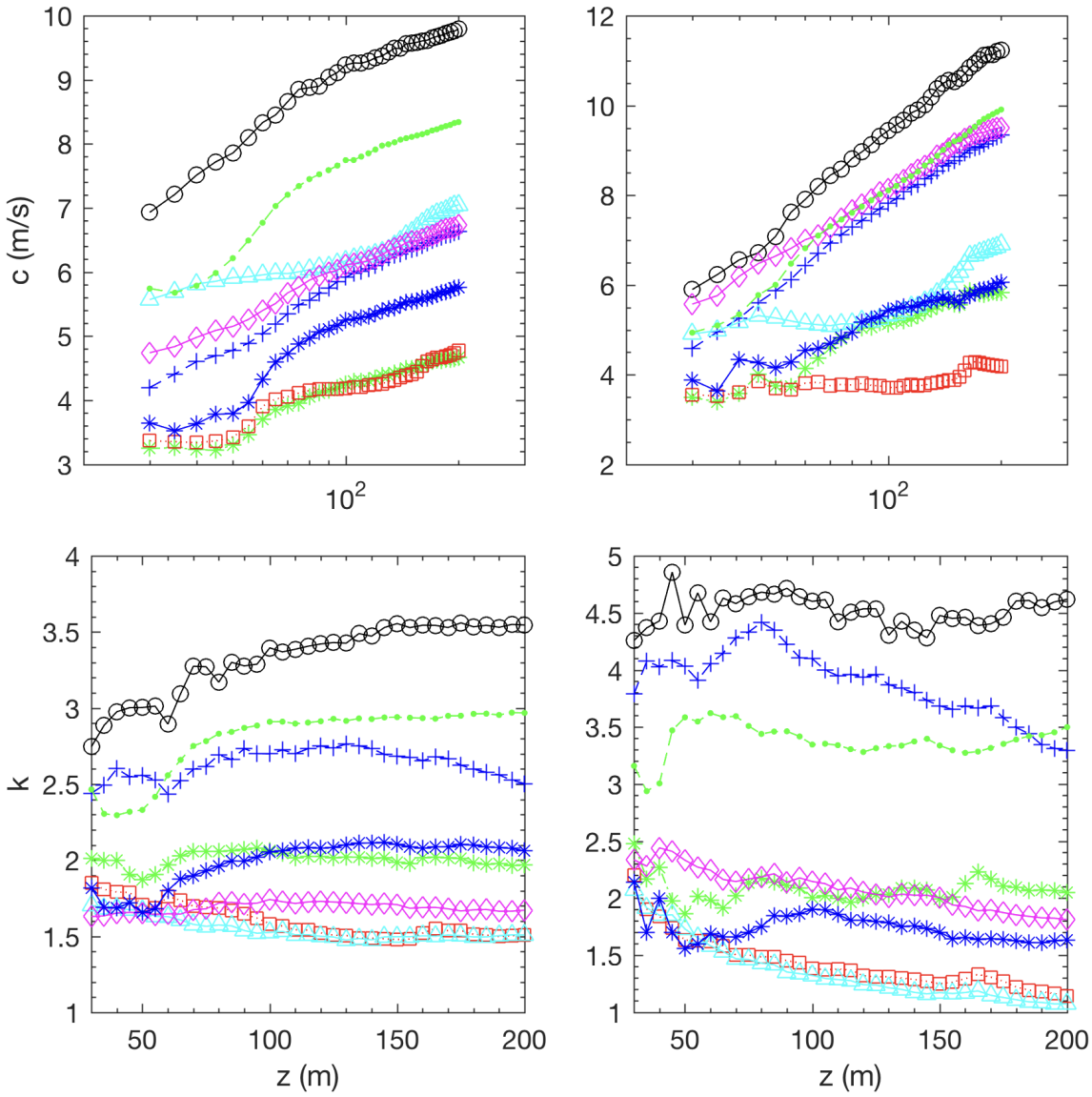

Figure 2.9: Vertical variations of scale factor c and shape factor k of the Weibull distributions best-fitted using the measurement data near T75 turbine for different wind directions. Black solid line with circles: 0^o; Blue-dashed line with crosses: 45^o; Green dash-dot line with asterisks: 90^o; Red dotted line with squares: 135^o; Cyan solid line with triangles: 180^o; Magenta solid line with diamonds: 225^o; Blue solid line with asterisks: 270^o; Green dashed line with points: 315^o. Left figures: day measurement; Right figures: night measurement.

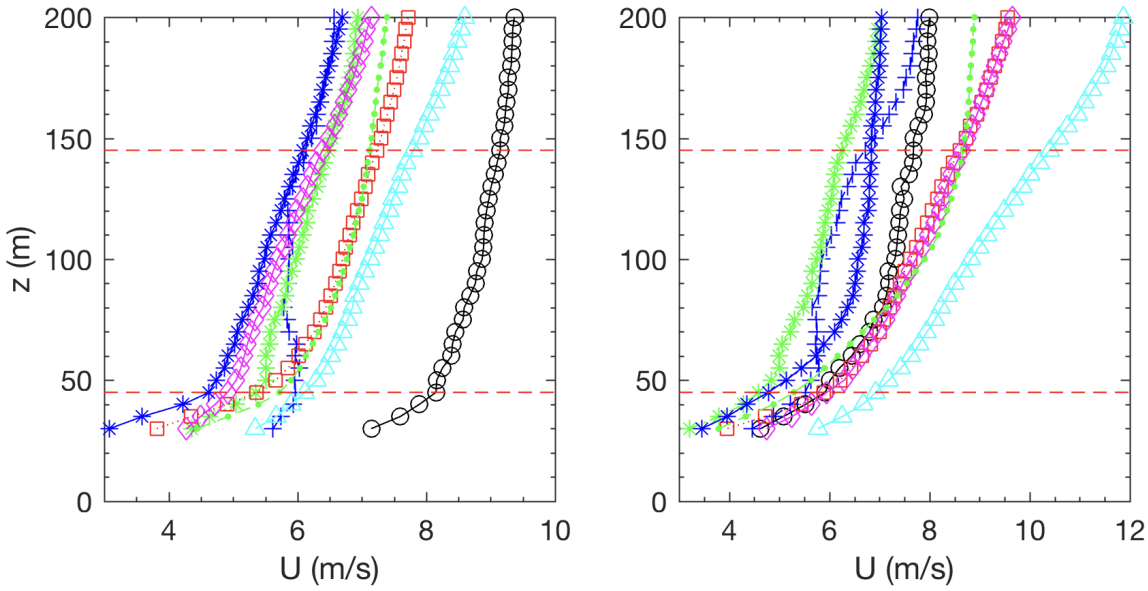

Figure 2.10: Vertical profiles for time-averaged wind speed for different wind directions for wind data measured near the T78 turbine location. Black solid line with circles: 0^o; Blue-dashed line with crosses: 45^o; Green dash-dot line with asterisks: 90^o; Red dotted line with squares: 135^o; Cyan solid line with triangles: 180^o; Magenta solid line with diamonds: 225^o; Blue solid line with asterisks: 270^o; Green dashed line with points: 315^o. Left figures: day measurement; Right figures: night measurement.

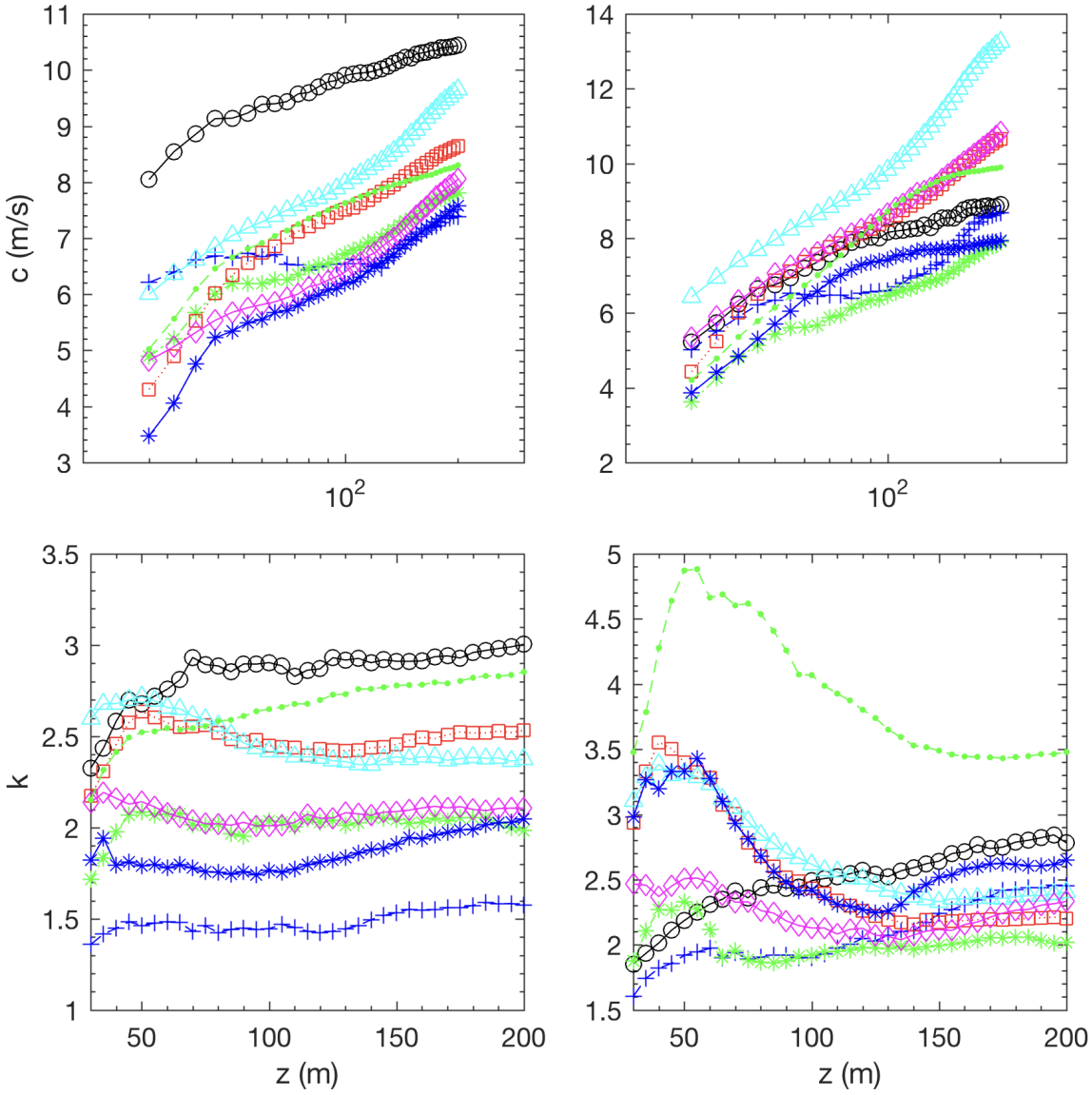

Figure 2.11: Vertical variations of scale factor c and shape factor k of the Weibull distributions best-fitted using the measurement data near T78 turbine for different wind directions. Black solid line with circles: 0^o; Blue-dashed line with crosses: 45^o; Green dash-dot line with asterisks: 90^o; Red dotted line with squares: 135^o; Cyan solid line with triangles: 180^o; Magenta solid line with diamonds: 225^o; Blue solid line with asterisks: 270^o; Green dashed line with points: 315^o. Left figures: day measurement; Right figures: night measurement.

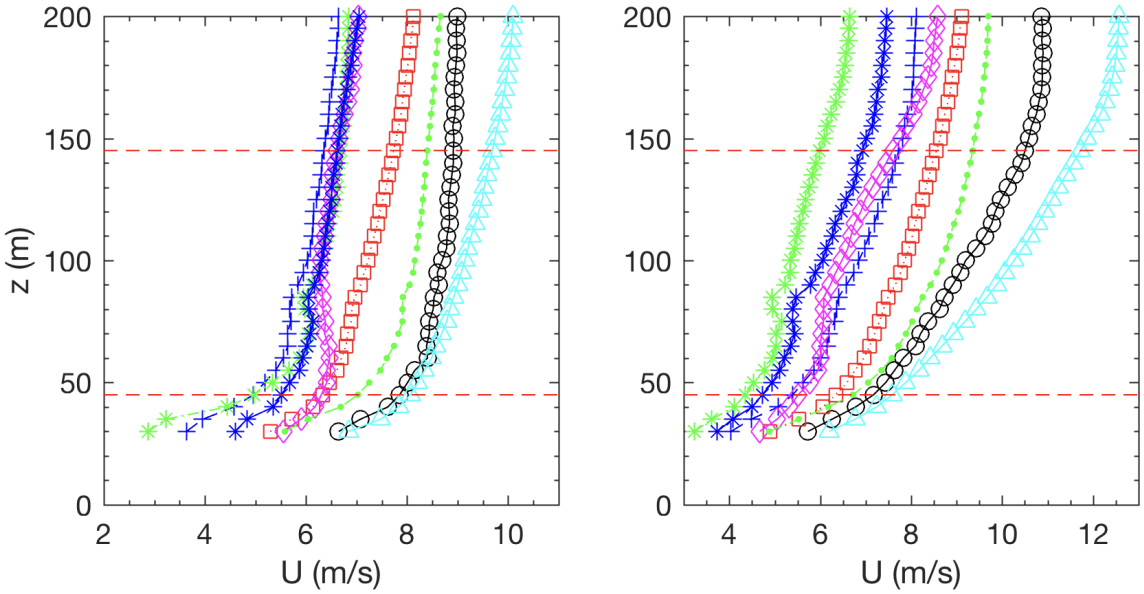

Figure 2.12: Vertical profiles for time-averaged wind speed for different wind directions for wind data measured near the T96 turbine location. Black solid line with circles: 0^o; Blue-dashed line with crosses: 45^o; Green dash-dot line with asterisks: 90^o; Red dotted line with squares: 135^o; Cyan solid line with triangles: 180^o; Magenta solid line with diamonds: 225^o; Blue solid line with asterisks: 270^o; Green dashed line with points: 315^o. Left figures: day measurement; Right figures: night measurement.

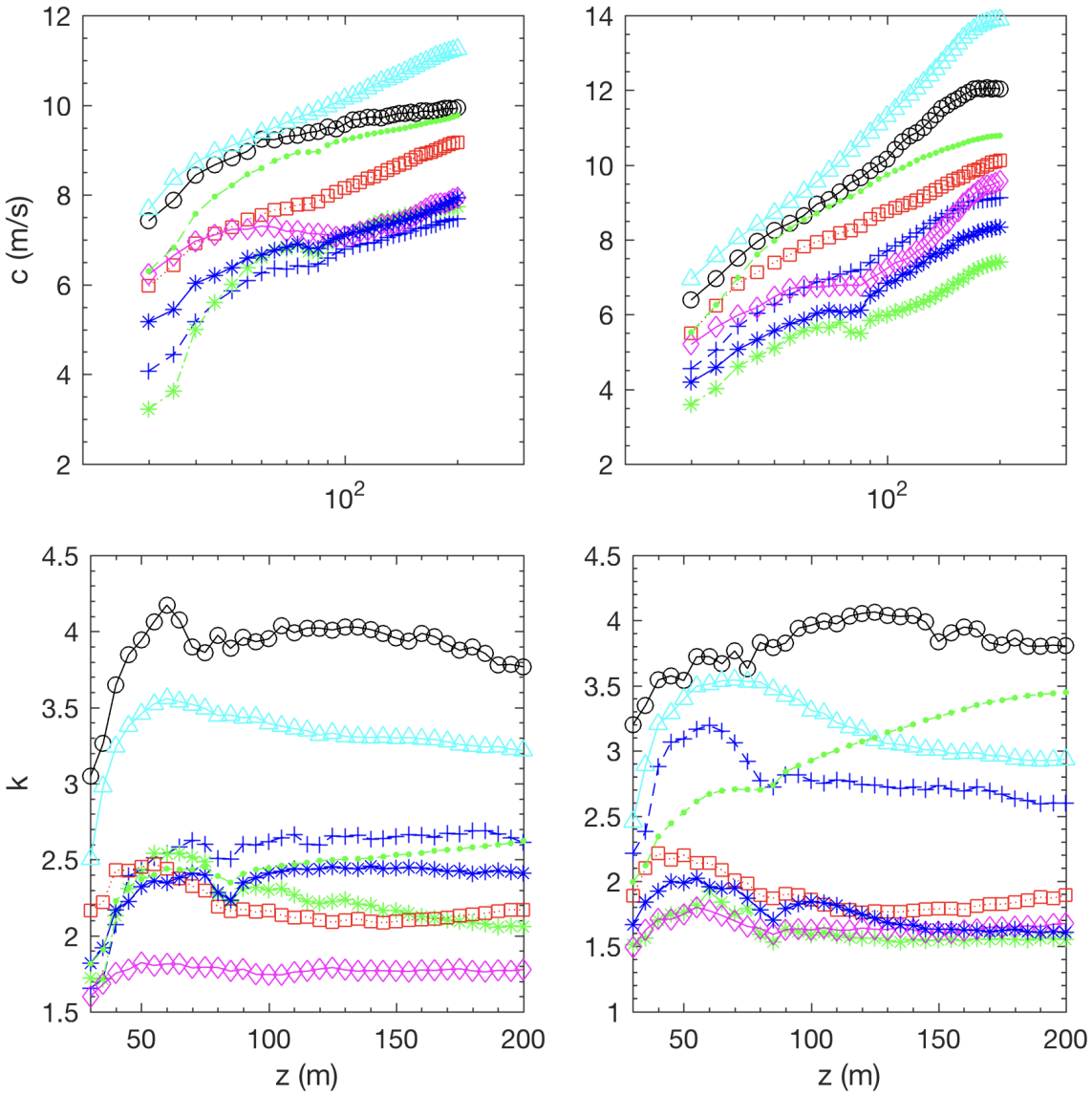

Figure 2.13: Vertical variations of scale factor c and shape factor k of the Weibull distributions best-fitted using the measurement data near T96 turbine for different wind directions. Black solid line with circles: 0^o; Blue-dashed line with crosses: 45^o; Green dash-dot line with asterisks: 90^o; Red dotted line with squares: 135^o; Cyan solid line with triangles: 180^o; Magenta solid line with diamonds: 225^o; Blue solid line with asterisks: 270^o; Green dashed line with points: 315^o. Left figures: day measurement; Right figures: night measurement.

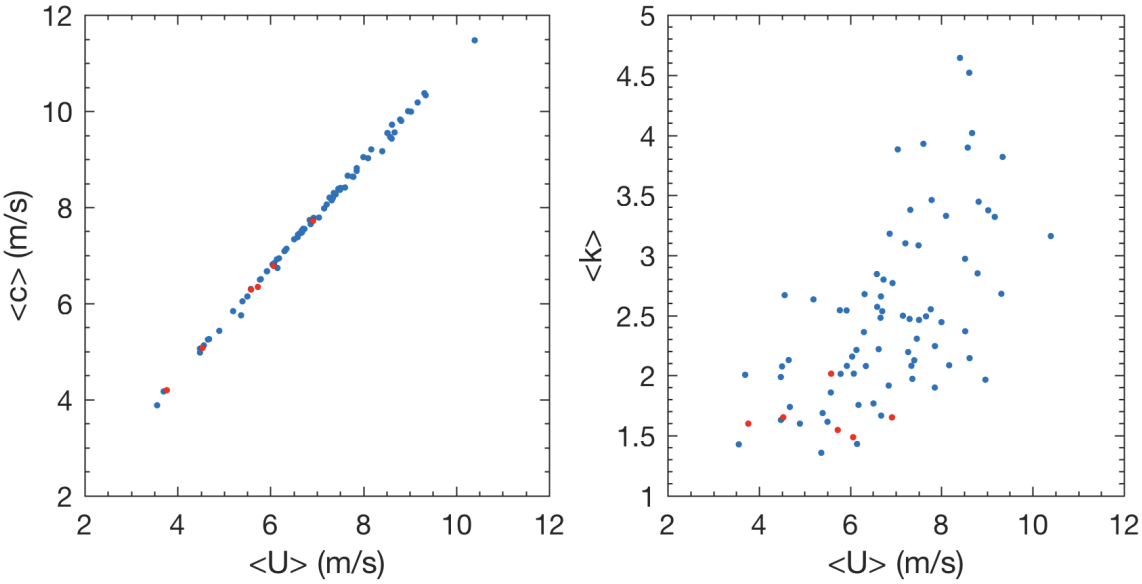

Figure 2.14: Variations of vertical averaged scale factor c (left) and shape factor k (right) as a function of vertical averaged wind speed. The red points show the measurements with turbine wakes.

are observed when wind blows from certain directions for different measurement locations. We compared the best-fitted Weibull distributions with the measurements. We found that the scale factor of Weibull distribution linearly increases with wind speed for both measurements with and without wakes. The overall trend of the shape factor also shows its increase with wind speed but the data are much scattered. It is also noticed that the shape factors from the measurements with wakes are less than those without wakes.

References

Project Status : This project is ahead of schedule and within budget.